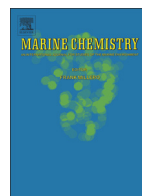




Contents lists available at SciVerse ScienceDirect

Marine Chemistry

journal homepage: www.elsevier.com/locate/marchem

Karstic groundwater discharge and seawater recirculation through sediments in shallow coastal Mediterranean lagoons, determined from water, salt and radon budgets

Thomas C. Stieglitz ^{a,b,c,*}, Pieter van Beek ^c, Marc Souhaut ^c, Peter G. Cook ^d

^a School of Engineering & Physical Sciences, James Cook University, Townsville QLD 4811, Australia

^b Centre for Tropical Water and Aquatic Ecosystem Research, James Cook University, Townsville QLD 4811, Australia

^c Laboratoire d'Etudes en Géophysique et Océanographie Spatiales UMR 5566, 14 av. Edouard Belin, 31400 Toulouse, France

^d CSIRO Water for a Healthy Country and National Centre for Groundwater Research and Training, School of the Environment, Flinders University, Adelaide SA 5001, Australia

ARTICLE INFO

Available online xxxx

Keywords:

Groundwater
Seawater recirculation
Lagoon
Radon
Water budget
Mediterranean
La Palme lagoon
Salses-Leucate lagoon
Thau lagoon

ABSTRACT

Groundwater discharge to coastal water bodies is increasingly recognised to contribute significantly to coastal water and solute budgets. In order to evaluate the discharge of low-salinity groundwater of karstic origin and of recirculation of seawater through sediments into Mediterranean lagoons, a study was carried out in La Palme, Salses-Leucate and Thau lagoons on the French Mediterranean coastline in the dry summer months 2009, using radon and salinity as tracers.

Whereas Salses-Leucate lagoon receives significant fluxes of karstic low-salinity groundwater, in La Palme and Thau lagoons, karstic groundwater fluxes are small, and have little effect on the lagoons' radon balance. A simultaneous water, salt and radon budget of the small La Palme lagoon (ca 50 ha surface area and 0.6 m mean depth) was used to simulate average salt and radon concentration over a one month period. The results indicate that despite its small flux (0.8–1.2% of lagoon volume per day) the discharge of low-salinity karstic groundwater contributes significantly to maintaining salinity lower than seawater in the seasonally closed lagoon, but makes only a minor contribution (7–18%) to the radon budget.

Wind-driven seawater recirculation through sediments on the other hand is a major contributor, estimated at 22–60% of total radon fluxes to the lagoon, equivalent to a water flux of 1.4–7.0% of lagoon volume day^{−1}. The remaining balance of Radon is supplied by diffusion and in-water production from decay of its parent nuclide. Using a stand-alone radon model without considering a water and salt balance would have considerably overestimated the flux of groundwater of karstic origin.

Radon can be regarded as a proxy for other dissolved solutes such as nutrients and contaminants transported with groundwater and seawater recirculation fluxes. Nutrient and contaminant enrichment of sediments in Mediterranean lagoons is well documented. Wind-driven seawater recirculation through these sediments as documented in this study may remobilise these nutrients and contaminants. It may thus play a considerable role in lagoonal biogeochemical budgets, and may require consideration in water quality management in Mediterranean coastal lagoons.

Crown Copyright © 2013 Published by Elsevier B.V. All rights reserved.

1. Introduction

Supratidal, intertidal and submarine groundwater discharge is increasingly recognised to contribute significantly to coastal water and solute budgets. In particular sub-tidal or submarine groundwater discharge (SGD) has been documented to impact many shorelines of the

world (Moore, 2010). Water budgets of enclosed and semi-enclosed water bodies such as estuaries and coastal lagoons can be particularly affected by groundwater inflow, due to reduced mixing with offshore waters and greater water residence times (e.g. Johannes and Hearn, 1985). A significant body of literature documents fresh groundwater inputs into lagoonal systems ranging from a few per cent to 100% of total freshwater inputs across different climatic zones of the world (e.g. Smith et al., 1999). Commonly the discharge of land-derived fresh (or low-salinity) groundwater from terrestrial sources is of interest, and many lagoon studies are based on volumetric water balance or hydrological modelling (e.g. Kjerfve, 1994; Martínez-Alvarez et al., 2011). In this paper, the term 'groundwater' is used for low-salinity water of karst origin, and excludes seawater recirculation through sediments,

* Corresponding author at: Laboratoire des sciences de l'environnement marin UMR 6539, Institut Universitaire Européen de la Mer, Université de Bretagne Occidentale, 29280 Plouzané, France. Tel.: +33 2 98 49 86 54.

E-mail addresses: Thomas.Stieglitz@jcu.edu.au (T.C. Stieglitz), vanbeek@legos.obs-mip.fr (P. van Beek), marc.souhaut@legos.obs-mip.fr (M. Souhaut), peter.cook@flinders.edu.au (P.G. Cook).

contrary to the common terminology in the ocean science community which commonly regards both processes as groundwater (e.g. Moore, 2010).

Variations of salinity, temperature and nutrient discharge into a lagoon from either surface water or groundwater are important drivers of ecosystem functioning in shallow lagoons (Beklioglu et al., 2007). Over the past 50 years, many Southern European lagoons have experienced severe water quality problems as a result of increasing anthropogenic pressures, in particular mass tourism and substantial agricultural production in the catchment areas (Viaroli et al., 2005; Zaldívar et al., 2008). The European Union's Water Framework Directive requires European countries to establish and monitor status of their water bodies. Whilst the Directive is less well implemented in coastal than in inland waters, significant effort is now directed at the monitoring, maintenance and restoration of ecosystem functioning of coastal lagoon systems in the Mediterranean (e.g. Andral and Sargian, 2010).

Successful water quality management requires a good understanding of the basic water exchange processes occurring in a water body. Groundwater is recognised as a pathway for nutrients and contaminants to the coastal zone (Johannes, 1980; Slomp and Van Cappellen, 2004), and in recent years, groundwater discharge into several lagoons along the European Mediterranean coastline has been documented using natural radioactive tracers (e.g. Rapaglia et al., 2009; Rodellas et al., 2012), including groundwater discharge from karstic aquifers (e.g. Povinec et al., 2006; Garcia-Solsona et al., 2010).

Lagoonal systems represent ca. 50% of the western part of France's Mediterranean coastline. They are of high economic importance and conservation value (Troussellier and Bacher, 2006). Whilst low-salinity groundwater is known to discharge from karstic aquifers into many lagoons on this coastline (Fleury et al., 2007), little information is presently available on its effect on lagoonal water and solute budgets. Importantly, currently no information exists on lagoon-internal recirculation of lagoon water through sediments. Considering the well-documented enrichment of nutrients in the sediments of some lagoons (e.g. De Casabianca et al., 1997; Galgani et al., 2009), a better understanding of the potential for seawater recirculation through lagoonal sediments is required to evaluate the potential importance of this sediment-water exchange process on biogeochemical budgets.

The purpose of the study reported here is to document the inflow of low-salinity groundwater discharge from the extensive karst aquifers to

the coastal lagoons, and to gain an order-of-magnitude understanding of the relative importance of this karstic groundwater and lagoon water recirculation through sediments. The naturally occurring radioactive isotope ^{222}Rn and salinity are used as tracers. Radon is frequently employed to determine groundwater input to the coastal ocean, rivers and other surface water bodies (e.g. Burnett and Dulaiova, 2003; Cook et al., 2003; Burnett et al., 2006; Povinec et al., 2008). It is typically elevated in groundwater relative to surface waters by 2–3 orders of magnitude, and delivered to coastal waters through four main mechanisms, (1) groundwater discharge, (2) river discharge, (3) recirculation of seawater through sediments, and (4) diffusion from sediments.

In 2009, concurrent spatial mapping of the distribution of radon and salinity in the Mediterranean lagoons of La Palme, Salses-Leucate and Thau elucidated the distribution of groundwater discharge into the lagoons. For La Palme lagoon, contributions from karstic groundwater and recirculated seawater to the radon budget are estimated from a simultaneous water, salt and radon balance.

1.1. Study area

La Palme, Salses-Leucate and Thau lagoons are located on the western French Mediterranean coastline (Fig. 1). The hydrogeology of this region is dominated by the karstic rocks and aquifers of the coastal uplands (Fleury et al., 2007). Groundwater discharges perennially from isolated, sometimes high-flow springs associated with fractures in the karst directly into the ocean or into lagoons, including at the study sites La Palme, Salses-Leucate and Thau lagoons (Wilke and Boutière, 2000; Fleury et al., 2007).

In the region's Mediterranean climate, little to no rain falls during the summer months. Tidal water level variations in the Mediterranean are small with maximum amplitudes of 0.4 m, and mixing of coastal waters in this region is driven primarily by wind and air pressure changes. The region is well-known for strong north-westerly winds called 'Tramontane' or 'Le Cers', regular exceeding 10 m s^{-1} .

1.1.1. La Palme lagoon

La Palme lagoon is a small water body (500 ha surface area) of considerable conservation value due its high diversity in aquatic habitats. Despite episodic eutrophication events, its extraordinary ecological diversity is recognised internationally by its classification



Fig. 1. Study site locations (a) and site map with bathymetry (in m) of the principle study site La Palme lagoon (b). Water level monitoring sites are marked with WL. Streams marked with white lines are only flowing during winter rains.

under the RAMSAR convention; it is listed in the French environmental protection program Natura 2000 as site of outstanding ecological value and listed as reference site for the European Framework Directive for Water Quality Protection.

Groundwater discharge from the regional karst aquifer occurs throughout the year in the northern section of the lagoon. A captured spring feeds a nearby 'lavoir' (traditional wash basin), which is connected with the lagoon via a small stream flowing through a perennial wetland, which itself is noted for its high diversity in natural habitats. The combined discharge from this spring via the small stream and from the aquifer underlying the wetland is here considered as groundwater flow.

Small streams seasonally discharge freshwater into the lagoon. During the summer months, there is no surface water inflow associated with these streams due to the small catchment to the lagoon (Wilke and Boutière, 2000). Salt evaporation ponds adjacent to the lagoon produced salt until the 1970s, and are no longer in operation. A small number of drainage channels connect the ponds to the lagoon, through which they drain during periods of high rainfall; exchange between them and the lagoon does not persist in the dry summer months (Wilke and Boutière, 2000).

The lagoon is shallow, with a mean and maximum water depth of 0.6 m and 1.5 m respectively (Fig. 1). It is vertically well mixed due to wind-driven mixing common in shallow lagoons (Spaulding, 1994). It is seasonally connected with the Mediterranean Sea via a small opening ('grau') in the coastal sand spit. In the summer months, this grau is closed. Exchange with the ocean is further restricted by a road dike and a railway dike which are intersected by only one small bridge each, allowing only minimal exchange (Fig. 1). In addition, much of the southern section referred to as 'Les Seches' ('the dry') is less than 0.2 m deep on average, and is known to partially fall dry in some years. The combination of these effects results in an effective separation between northern and southern lagoon during the summer months, with only a small exchange between the two sections.

1.1.2. Salses-Leucate & Thau lagoons

Salses-Leucate and Thau lagoons are considerably larger in surface area than La Palme lagoon, and have average depths of 1.7 m and 4.5 m respectively. Both lagoons are important site for shellfish farming, in particular of oysters and mussels; oyster production in Thau lagoon accounts for ca. 10% of France's oyster consumption. These lagoons are under significant anthropogenic pressure, and eutrophication and algal blooms outbreaks are common (e.g. De Casabianca et al., 1997; Andral and Sargian, 2010). Salses-Leucate and Thau lagoons receive low-salinity groundwater input from the well-known karstic spring complexes of Font Dame/Font Estramar and La Vise respectively. Discharge estimates for Font Estramar and Font Dame are $1\text{--}10\text{ m}^3\text{ s}^{-1}$ and $1\text{--}5\text{ m}^3\text{ s}^{-1}$ respectively, whereas La Vise discharges only a few 100 L s^{-1} into Thau lagoon, at a depth of ca. 30 m (Aquilina et al., 2002; Fleury et al., 2007).

1.2. Materials & methods

1.2.1. Sample collection & analysis

Radon was continuously sampled and counted in situ using two electronic radon-in-air monitors (DurrIDGE RAD-7) in parallel. Surface water was pumped directly and continuously through a gas exchange membrane (Schubert et al., 2012a). Dissolved radon in seawater was purged into a closed air loop, which circulates through the monitors, to establish equilibrium between the circulating air and the continuously pumped seawater. The monitors count α -decays of ^{222}Rn daughters, and ^{222}Rn concentration is determined by discriminating the ^{222}Rn -daughter decays in energy-specific windows. The spatial distribution of ^{222}Rn was recorded by continuously sampling whilst slowly traversing the lagoon. Concurrently with radon, surface water salinity and temperature was

recorded with a laboratory-calibrated Hydrolab water quality sonde. Radon concentration in water was determined from the measured in-air-concentration after Schubert et al. (2012b), taking water salinity into account. Laboratory experiments have shown that this radon extraction using in-situ equilibration introduces a small lag time, which was corrected for by adjusting the time of measurement along the vessel track after Stieglitz et al. (2010). Sampling interval was five minutes, which resulted in a spatial resolution of better than 200 m, depending on boat speed.

The radon concentration of Mediterranean seawater was measured using the same method, and radon concentration of groundwater sources were determined by purging Radon from 250 ml sample bottles directly into a counter using the DurrIDGE RadH2O extraction system. Groundwater samples were collected without gas loss using submerged pumps from previously known springs representative for the underlying karst aquifer. In order to determine in situ production of radon in lagoon water from decay of its radioactive parent ^{226}Ra , 20–40 L samples of water were collected for analysis of ^{226}Ra concentration using low-background gamma spectrometry (van Beek et al., 2010). The ^{226}Ra concentration of lagoon sediment was determined by low-background gamma spectrometry of two representative oven-dried sediment samples (van Beek et al., 2010). In addition, an incubation experiment was carried out with one of these sediment samples. Ca. 17 g of sediment (dry weight) with a volume of 16 mL was incubated in a 250 mL bottle filled with water without headspace. The sediment was incubated for 6 weeks and the bottle was periodically shaken. The radon concentration in water was then measured directly using the DurrIDGE RadH2O system. The radon production rate γ can be calculated as

$$\gamma = C_{\text{incubation}} \lambda \frac{R_{\text{lab}}}{R_{\text{field}}} \quad (1)$$

where $C_{\text{incubation}}$ is the measured concentration in the incubation chamber [Bq m^{-3}], and R_{lab} and R_{field} are ratios of volume of water to sediment in the incubation chamber (lab) and in the field (which is a function of the porosity) respectively. One-sigma uncertainties are reported for all radionuclide concentrations.

In La Palme lagoon, radon and salinity data were collected on 26 June, 3 July, 15 July and 30 July 2009. On 3 July the entire lagoon was surveyed. On the other dates only the northern section was investigated, mainly because the low water level in the transition between northern and southern lagoon prevented sample collection. For each date, a volume-weighted average radon concentration and salinity for the northern section of the lagoon was calculated from grids interpolated by kriging at 50 m spatial resolution. ^{226}Ra was sampled on 26 June 2009, and a volume-weighted averaged determined similarly.

Lagoon water level was recorded continuously at the northern and southern end of La Palme lagoon in 10 min intervals from 20 June to 30 July 2009, together with atmospheric pressure. Water levels were corrected for atmospheric variation, and the difference between water level at northern and southern end of the lagoon calculated. Hourly rainfall and wind data at the nearby station 'Leucate' was extracted from the database of the French meteorological service. Surface area and volume of the lagoon was calculated in a GIS from data provided by the Parc naturel régional de la Narbonne (Anonymous, 2007), corrected with data measured by echosounder along the sampling track.

In Salses-Leucate & Thau lagoons, concurrent transects of salinity and radon concentration were recorded on 10 June and 21 July 2009 respectively. Data from these two lagoons are insufficient to construct adequate radon balances, but are nevertheless useful to obtain a qualitative understanding of groundwater processes contributing to the lagoons' salinity and radon budgets and are thus presented herein.

1.2.2. Lagoon water, salt and radon balance

In order to determine groundwater inflow into La Palme lagoon, simultaneous water, salt and radon balances are constructed. The

lagoon consists of two sections with only a small exchange between them, and the water, salt and radon balances are calculated for the northern section only, in which salinity and radon data was collected on four different dates (Fig. 2).

If there is no surface water inflow and no outflow, then the evaporative loss of water must be balanced by input of water from groundwater and precipitation. Thus the surface water balance for the northern section of the lagoon is

$$\frac{\partial V_N}{\partial t} = Q_g + PA_N - EA_N - J_{NS} \quad (2)$$

where V_N is the volume of the northern section [m^3], Q_g is the groundwater inflow rate [$\text{m}^3 \text{ day}^{-1}$], P is the precipitation rate [$\text{m}^3 \text{ day}^{-1}$], E is the evaporation rate from the water surface [$\text{m}^3 \text{ day}^{-1}$], A_N is the surface area of the northern section [m^2] and t is time [days]. The additional flux J_{NS} [$\text{m}^3 \text{ day}^{-1}$] from northern to southern section accounts for water exchange between sections. It is a loss term for the northern section, assuming groundwater inflow only occurs in the northern section (and provided $E > P$), and equals the evaporative loss minus precipitation in the southern lagoon section:

$$J_{NS} = EA_S - PA_S \quad (3)$$

where A_S is the surface area of the southern lagoon section.

The salt balance for the northern section of the lagoon is

$$\frac{\partial SV_N}{\partial t} = Q_g S_g - J_{NS} S + D_{NS} \Delta S_{NS} \quad (4)$$

with S the mean salinity (unit-less) of the northern section of the lagoon and S_g the groundwater salinity. Note that salinity is here taken

equivalent to salt concentration. An additional dispersive exchange flux D_{NS} [$\text{m}^3 \text{ day}^{-1}$] between the northern section and the southern section must be considered, allowing for flux of salt (and radon) from the southern section to the northern section. ΔS_{NS} is the difference in salinity at the boundary between northern and southern lagoon section. Note that this dispersive exchange D_{NS} between the two sections of the lagoon has a net opposite direction to J_{NS} (from south to north) and does not have a net influence on the water balance in Eq. (2).

Similarly, the radon mass balance is

$$\frac{\partial CV_N}{\partial t} = Q_g C_g + P_{Ra226} + (F_{diff} + F_{recirc}) A_N - k A_N C - \lambda V_N C - J_{NS} C + D_{NS} \Delta C_{NS} \quad (5)$$

with the mean concentration of radon within the northern lagoon C [Bq m^{-3}], the concentration in groundwater inflow C_g [Bq m^{-3}], the in-water production of radon by radioactive decay of its parent ^{226}Ra P_{Ra226} [Bq day^{-1}], the flux per unit area from the underlying sediments due to diffusion F_{diff} and seawater recirculation F_{recirc} [$\text{Bq m}^{-2} \text{ day}^{-1}$], surface area and volume of the northern section of the lagoon A_N and V_N respectively, the gas transfer velocity k [m day^{-1}], and the radioactive decay constant λ [day^{-1}]. ΔC_{NS} is the difference in radon concentration at the boundary between northern and southern lagoon section.

The change in concentration with time is calculated by

$$\frac{\partial CV_N}{\partial t} = C \frac{\partial V_N}{\partial t} + V_N \frac{\partial C}{\partial t} \quad (6)$$

where C represents either radon concentration or salinity. Assuming a constant water level and volume in the northern section of the lagoon

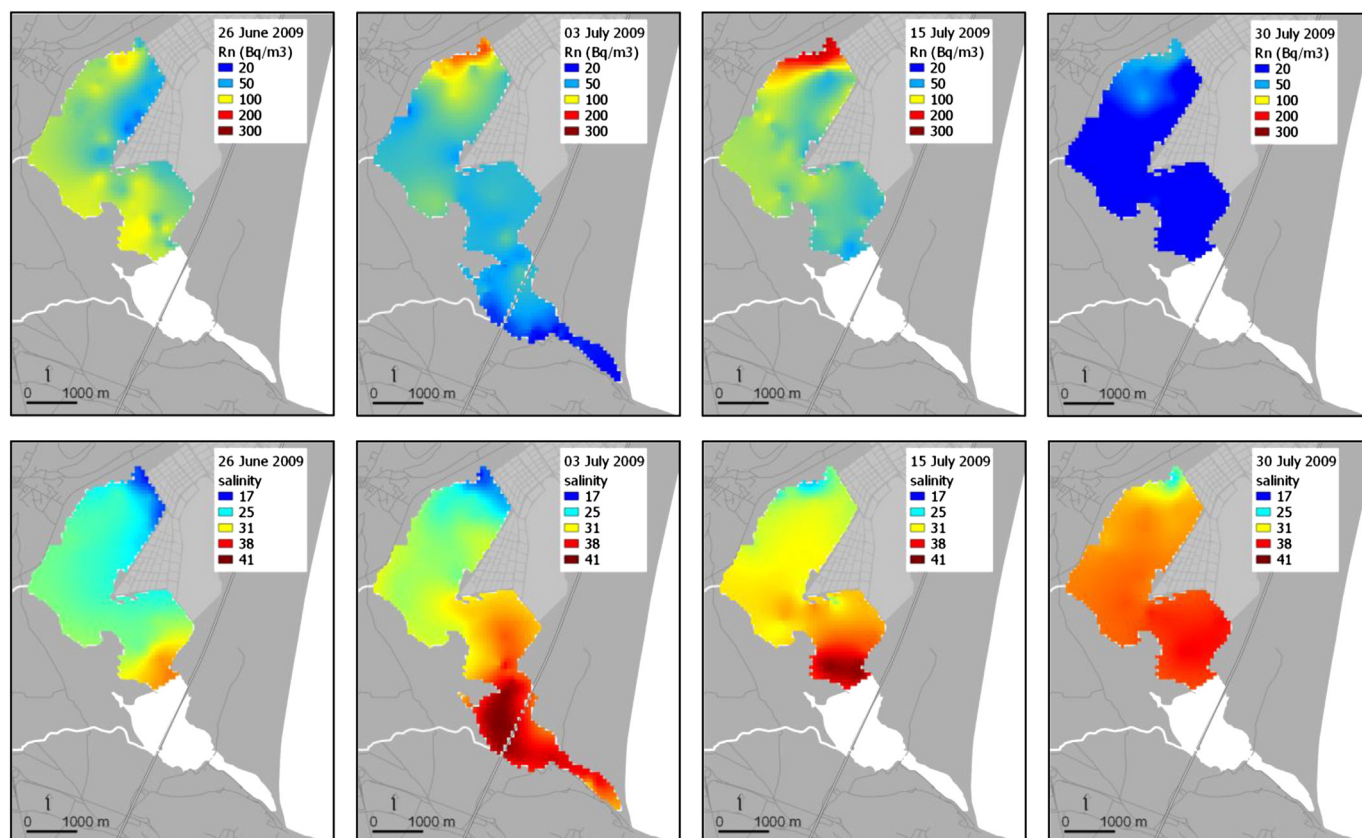


Fig. 2. Interpolated radon concentration and salinity in June/July 2009 in La Palme lagoon. Non-linear colour schemes were applied to emphasise the distribution pattern in the visualization. (For interpretation of the references to colour in this figure legend, the reader is referred to the web version of the article.)

during the observation period ($dV_N/dt = 0$), the change in radon concentration is therefore given by

$$\frac{dC}{dt} = \frac{1}{V_N} (Q_g C_g + P_{Ra226} + (F_{diff} + F_{recirc}) A_N - k A_N C - \lambda V_N C - J_{NS} C + D_{NS} \Delta C_{NS}) \quad (7)$$

Eqs. (2) and (4) are solved analytically, and uncertainties are calculated by propagation of uncertainties in the measured parameters. Eq. (7) is solved numerically.

1.2.3. Estimation of seawater recirculation through sediments in the hypersaline zone of the lagoon – an alternative approach

In this section, an alternative approach to determining the recirculation of seawater through lagoon sediments is presented. This process is analogous to hyporheic exchange in freshwater systems, i.e. circulation through the bed of a freshwater stream. Cook et al. (2006) developed a steady-state solution to determine hyporheic exchange in rivers, which can also be applied to seawater recirculation through lagoon sediments under investigation here. A shallow zone in the sediment (analogous to the hyporheic zone) is assumed to be flushed, with a net water flux across the sediment water interface of zero. The steady state mass balance of the flushed sediment per unit area is:

$$q(C - C_I) + \gamma h \theta - \lambda h C_I \theta = 0 \quad (8)$$

where q is the flux into and out of the sediment, C and C_I the radon concentration of the overlying water and interstitial water respectively, γ the production rate of radon within this zone and h and θ are the zone's thickness and porosity respectively (Cook et al., 2006). Following Cook et al. (2006), the mean residence time T of seawater within the sediment is

$$T = h\theta/q \quad (9)$$

Rearranging Eq. (8) and substituting the depth of the exchange zone h by Eq. (9) yields

$$C_I = \frac{C + \gamma T}{1 + \lambda T} \quad (10)$$

Considering a body of water in steady-state where the only source of radon is water recirculation through sediments, and where there is no loss other than radioactive decay and gas loss, then the radon mass balance of this water is

$$qC_I - qC - \lambda dC - kC = 0 \quad (11)$$

where d is water depth. Combining Eqs. (10) and (11) allows the calculation of the flux across the sediment–water interface with unit $m^3 \text{ day}^{-1} \text{ m}^{-2}$

$$q = \frac{C(\lambda d + k)}{\frac{C + \gamma T}{1 + \lambda T} - C} \quad (12)$$

These equations can be applied under conditions where radon supply from groundwater is negligible.

2. Results

2.0.1. Field data

The distribution of radon and salinity in La Palme lagoon clearly indicates a low salinity/high radon source in the far north of the lagoon (Fig. 2). Generally, radon concentration decreases and salinity increases with distance from this source. Hypersaline conditions persist in the southern part of the lagoon (outside the model domain, see below). The distribution of both the radon concentration and salinity, however, varies considerably with time. The significantly reduced radon concentration on

30 July during periods of high wind speed is particularly striking (Table 1; Fig. 2). Average salinity increases (linearly) with time, indicating that water loss from evaporation dominates over dilution with low-salinity groundwater (Table 1; Fig. 3). The lagoon, therefore, cannot be considered to be in a steady state with respect to radon and salinity.

For most of the observation period, wind speed remained below 10 m s^{-1} , but showed strong diurnal variability. During the last week of observation, multiple strong wind events occurred (Fig. 5c). Typical for a closed lagoon, the water level in the lagoon is not affected by semi-diurnal tides, but is strongly influenced by wind speed. A wind-driven periodic water level variation with approximately daily frequency is evident in the relative water level data (Fig. 5b). Note that the comparatively large wind-driven water level variability masks absolute changes in water level and thus lake volume. Accurate absolute water level variations cannot be calculated from this data.

The average concentration of the parent nuclide ^{226}Ra was calculated in a similar fashion as ^{222}Rn , i.e. as volume-weighted average of 13 samples approximately evenly distributed in the northern lagoon to be $38.6 \pm 0.4 \text{ Bq m}^{-3}$. This value is similar to concentrations found in comparable coastal settings by Rodellas et al. (2012). It is reasonable to assume that the average concentration of this long-lived radionuclide does not change significantly with time over the 35 day model period.

^{226}Ra concentration of two representative sediment samples was $35.8 \pm 0.54 \text{ Bq m}^{-3}$ and $28.2 \pm 0.46 \text{ Bq m}^{-3}$. The radon concentration measured at the end of the incubation experiment was $700 \pm 240 \text{ Bq m}^{-3}$ at a water to sediment ratio R_{lab} of 234 mL to 16 mL. Using Eq. (1) and a typical water to sediment ratio in the lagoon of $R_{field} = 0.67$ (sediment porosity of 0.4), a production rate γ of $2780 \pm 950 \text{ Bq m}^{-3} \text{ day}^{-1}$ is thus calculated.

Similar to the observations in La Palme lagoon, in-water radon concentration in Salses-Leucate lagoon decreases and salinity increases with distance from the Font Estramar/Font Dame spring complex on the western shore. Despite lack of freshwater input from streams during the summer months, lagoon salinity remains below seawater salinity of 37.1, indicating substantial influence of the low-salinity springs (Fig. 1). In Thau lagoon, radon concentration is greatly reduced in surface waters in comparison to La Palme and Salses-Leucate lagoons, except in the channel of the Canal Du Midi at the southern end of the lagoon. The highest radon concentration of 2040 Bq m^{-3} was found in a sample collected by diving at 30 m depth at the outlet of La Vise spring (salinity of 1.4; Table 1).

2.0.2. Water and salt balance

Precipitation during the observation period was minimal, with 0.4 mm, 0.2 mm and 4.6 mm recorded on 02/07/09, 04/07/09 and 15/07/09 respectively, and no precipitation on other dates. It is considered to have a negligible influence on water and salt budgets, and is thus not included further, i.e. $P = 0$ in Eq. (2)).

Table 1

Measured volume-weighted average salinity and radon concentration in La Palme lagoon (top) and salinity and radon concentrations of groundwater sources and ocean water (bottom).

Location	Date	S	C (Bq m ⁻³)		
			Min	Mean	Max
La Palme lagoon N	26/06/2009	26.7	57	72	87
	03/07/2009	28.9	52	63	73
	15/07/2009	31.5	65	76	87
	30/07/2009	34.7	13	19	25
Lavoir (La Palme)	26/06/2009	7.3		1600 ± 200	
Font Estramar	20/07/2009	5.1		8540 ± 580	
(Salses-Leucate)					
La Vise (Thau)	22/07/2009	1.4		2040 ± 140	
Mediterranean Sea		37.1		12 ± 3	

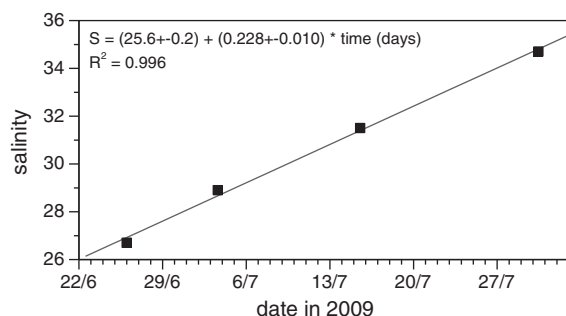


Fig. 3. Volume-weighted average salinity measured in La Palme lagoon.

Firstly, a water balance is constructed (Eq. (2)). This is a frequently used approach which yields robust results in small enclosed and semi-enclosed lagoons (e.g. Kjerfve, 1994). It is assumed that the volume of the lagoon is constant with time during the observation period ($dV/dt = 0$ in Eq. (2)), as well as the evaporation rate E and the groundwater inflow rate Q_g . These assumptions are consistent with the observed near linear temporal trend of average salinity (Fig. 3). Annual average evaporation from lagoons in the Mediterranean region is

3 mm day^{-1} (e.g. Obrador et al., 2008; Rodriguez-Rodriguez and Moreno-Ostos, 2006), with higher rates during the summer months. Because field work was carried out in the summer months, an evaporation rate E of $5 \pm 1 \text{ mm day}^{-1}$ is assumed, reflecting larger than average evaporation during summer (note that it will be seen later that E has little influence on the radon budget).

At constant lagoon volume (and no rainfall input), the groundwater inflow must balance the evaporative loss of water (from both parts of the lagoons). The groundwater inflow rate Q_g can be calculated from Eqs. (2) and (3) to be $(2.49 \pm 0.51) \times 10^4 \text{ m}^3 \text{ day}^{-1}$ or $(0.29 \pm 0.06) \text{ m}^3 \text{ s}^{-1}$ (Table 2).

Subsequently, the salt balance for the northern lagoon is constructed (Eq. (4)). At the calculated inflow rate of groundwater, which has a salinity of 7.3 ± 0.2 , a flux D_{NS} of $(1.17 \pm 0.26) 10^5 \text{ m}^3 \text{ day}^{-1}$ is required to achieve the observed increase of average salinity in the northern section (Fig. 3). This is equivalent to $4.6 \pm 1.0\%$ of northern lagoon volume per day.

2.0.3. Radon balance

Similar to Eqs. (2) and (4), Eq. (7) can be solved analytically when parameters are constant. Wind speed and associated loss of radon to the atmosphere however vary considerably during the 35 day observation

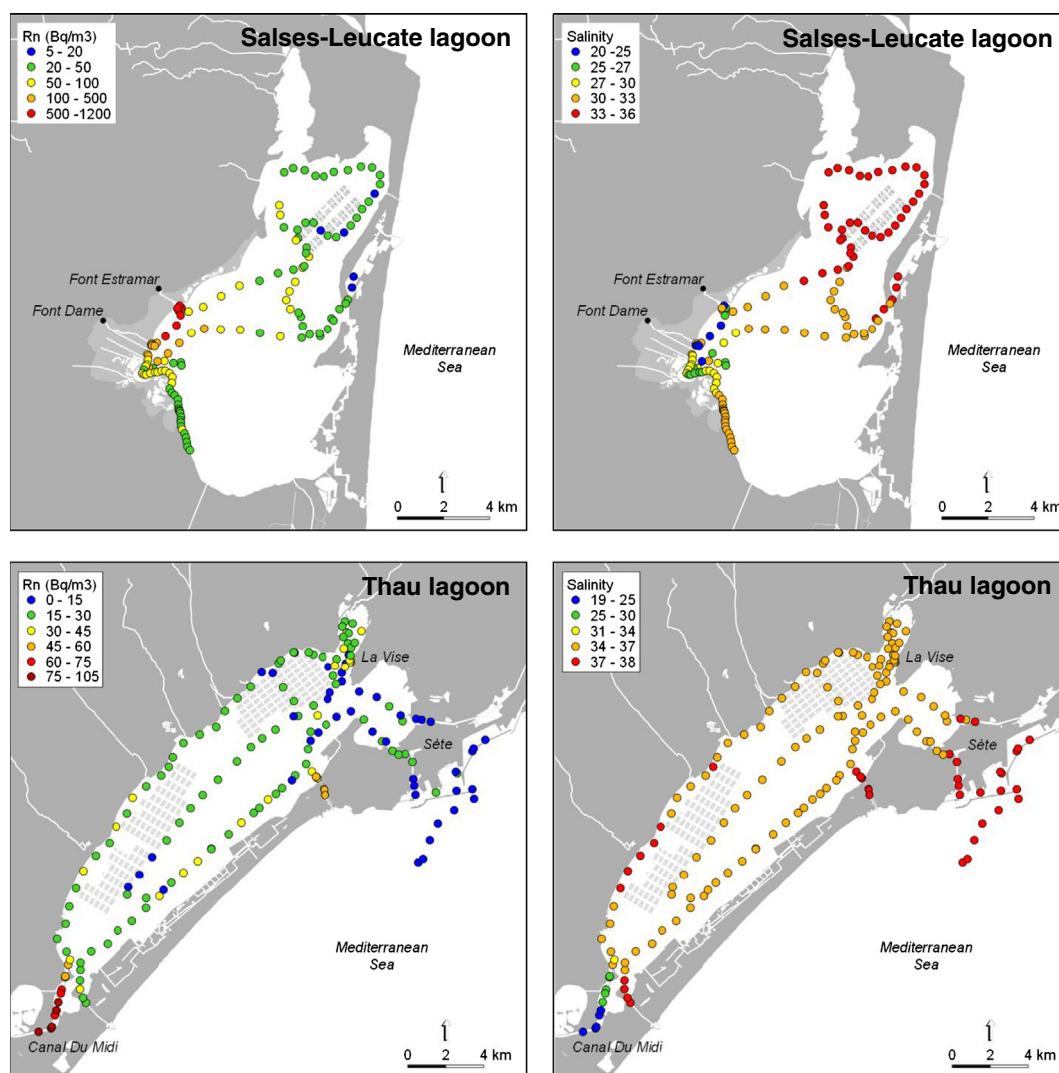


Fig. 4. Radon concentration and salinity in Salses-Leucate (top) and Thau (bottom) lagoons. Oyster rafts are shown in grey. The springs Font Estramar and Font Dame flow into Salses-Leucate lagoon via small streams, whereas 'La Vise' discharges directly into the northern sector of Thau lagoon in ca 30 m water depth.

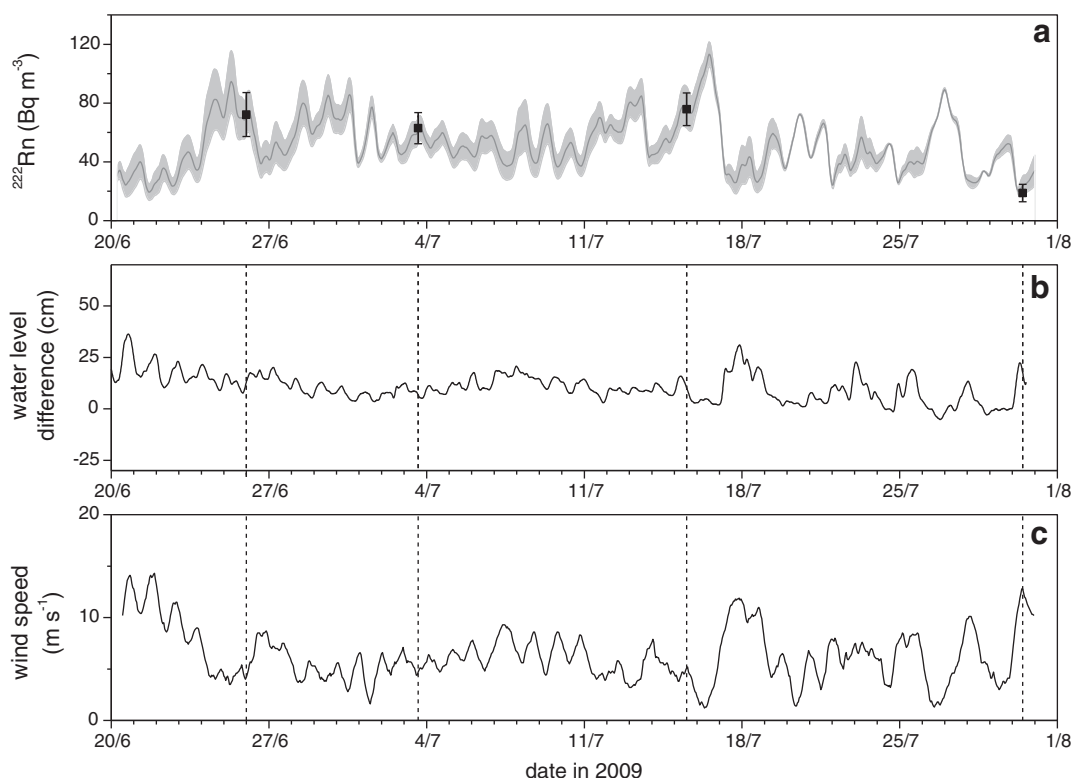


Fig. 5. Radon model results, showing modelled radon concentration and measured data on four dates (a), together with time series of measured water level difference (b) and wind speed (c) used to calculate seawater recirculation and gas loss term respectively.

period. Therefore, a numerical finite difference approach in one-hourly time steps similar to a model described in Cook et al. (2006) is taken, in order to allow for the parameters gas loss k and sediment flux F to vary with time. The values for Q_g and J_{NS} calculated in water and salt balance are used, together with other measured parameters (Table 2).

The diffusive flux F_{diff} [$\text{Bq m}^{-2} \text{d}^{-1}$] of radon from sediment can be calculated from an empirical linear relationship between sediment

^{226}Ra concentration and diffusive radon flux derived by Burnett et al. (2003)

$$F_{diff} = 0.495C_{226-sed} + 0.303 \quad (13)$$

where $C_{226-sed}$ is the ^{226}Ra concentration of the sediment [Bq kg^{-1}]. Using the average ^{226}Ra concentration of $32.0 \pm 0.5 \text{ Bq kg}^{-1}$ of the

Table 2

Parameters used to construct water, salt and radon balance of La Palme lagoon. 'Time series' denotes parameters that were not constant during the period for which the model was constructed.

Parameter	Description	Value	Unit	Source
<i>Water balance</i>				
E	Evaporation rate	0.005 ± 0.001	m day^{-1}	Estimated
A_N	Surface area N lagoon	$(3.79 \pm 0.19) 10^6$	m^2	Measured
A_S	Surface area S lagoon	$(1.19 \pm 0.06) 10^6$	m^2	Measured
Q_g	Groundwater inflow rate	$(2.49 \pm 0.50) 10^4$	$\text{m}^3 \text{day}^{-1}$	Calculated (Eq. (2))
<i>Salt balance</i>				
dS/dt	Change in salinity with time	0.229 ± 0.010	day^{-1}	Calculated
V_N	Volume N lagoon	$(2.61 \pm 0.13) 10^6$	m^3	Measured
S_g	Groundwater salinity (cf Table 1)	7.3 ± 0.2	–	Measured
J_{NS}	Exchange flux N–S	$(5.9 \pm 1.2) 10^3$	$\text{m}^3 \text{day}^{-1}$	Calculated (Eq. (3))
ΔS	Salinity difference N–S	5.0 ± 0.3	–	Measured
D_{NS}	Dispersive exchange flux S–N	$(1.17 \pm 0.26) 10^5$	$\text{m}^3 \text{day}^{-1}$	Calculated (Eq. (4))
<i>Radon balance</i>				
C_g	Groundwater Rn (cf Table 1)	1600 ± 200	Bq m^{-3}	Measured
C	Average lagoon Rn concentration	cf Table 1	Bq m^{-3}	Measured
P_{Ra226}	Rn production by Ra-226 decay	38.6 ± 0.4	$\text{Bq m}^{-3} \text{day}^{-1}$	Measured
F_{diff}	Rn diffusion flux from sediment	16.1 ± 4.4	$\text{Bq m}^{-2} \text{day}^{-1}$	Calculated (Eq. (13))
k	Gas transfer velocity	Time series	m day^{-1}	Calculated (Eq. (14))
λ	Radioactive decay constant	0.181	day^{-1}	Known
ΔC_{NS}	Radon conc difference N–S	-20 ± 5	$\text{Bq m}^{-3} \text{day}^{-1}$	Measured
F_{recirc}	Recirculation flux	Time series	$\text{Bq m}^{-2} \text{day}^{-1}$	Calculated (Eq. (7))

two sediment samples, a diffusive flux of $16.1 \pm 4.4 \text{ Bq m}^{-2} \text{ d}^{-1}$ is calculated.

The gas transfer velocity k depends on wind speed which is variable with time. Following MacIntyre et al. (1995), it can be determined as

$$k = 0.45 u_{10}^{1.6} (Sc/600)^{-0.5} \quad (14)$$

where u_{10} is wind [m s^{-1}] at 10 m height above the water surface (Fig. 5c), Sc is the temperature dependent Schmidt number for radon (840 at 23°C ; Wanninkhof et al., 2009). The number 600 is the Schmidt number for CO_2 at 20°C in freshwater, a common reference point. Modelled k ranges from 0.0 to 8.3 m day^{-1} as a result of a wind speed range from 0 to ca. 15 m s^{-1} .

The parameter F_{recirc} remains the only unknown (cf Table 2). This flux represents advective fluxes through sediments other than groundwater, i.e. seawater recirculation. Advection through sediments is driven by water level differences across the sediment. In many coastal settings, the primary driver is tidal pumping (e.g. Kim and Hwang, 2002). In La Palme lagoon however, tides do not affect water level variations, but wind-driven water level variations are evident (Fig. 5b). Therefore, here the flux F_{recirc} is considered to linearly vary with (wind-driven) water level difference between the northern and southern extension of the lagoon Δh (Fig. 5b):

$$F_{\text{recirc}} = f_{\text{recirc}} * Dh \quad (15)$$

The value f_{recirc} ($\text{Bq m}^{-2} \text{ day}^{-1} \text{ m}^{-1}$) is adjusted to obtain the best fit between observed and modelled radon concentration on the four observation dates.

Using mean values for all observed parameters from Tables 1 and 2, the best fit is obtained at $f_{\text{recirc}} = 392 \text{ Bq m}^{-2} \text{ day}^{-1} \text{ m}^{-1}$, resulting in an estimated total recirculation flux to the lagoon of $1.6 \times 10^8 \text{ Bq day}^{-1}$ respectively (Table 4), whereby the recirculation flux is reported as an average over the observation period 26 June–30 July 2009. Model results were constraint by additional runs, simulating minimum and maximum groundwater term. The maximum seawater recirculation flux was calculated by re-running the model using the minimum groundwater flux Q_g (mean minus uncertainty), together with minimum estimated C_g , P_{Ra226} and F_{diff} , and maximum estimated C_i , J_{NS} and ΔC to provide a ‘worst case’ constraint. Similarly, minimum seawater recirculation flux (at maximum groundwater flux) was modelled. This is considered a conservative approach in estimating the uncertainty of the model results. Results for minimum, mean and maximum groundwater flux are summarised in Table 3, and displayed in Fig. 5a.

2.0.4. Recirculation of lagoon water through sediments – an alternative approach

Incubation experiments provided an estimate of a radon production rate in lagoon sediments of $2780 \pm 950 \text{ Bq m}^{-3} \text{ day}^{-1}$. Together with this production rate, data collected from surface water in La Palme lagoon allows an alternative evaluation of the flux of radon to the lagoon from seawater recirculation through sediments,

Table 3
Comparison between data and model results for minimum, mean and maximum volume-averaged lagoon radon concentration of La Palme lagoon.

Date	Minimum		C (Bq m^{-3}) mean		Maximum	
	Data	Model	Data	Model	Data	Model
26/06/2009	57	57	72	70	87	82
03/07/2009	52	52	63	61	73	70
15/07/2009	65	64	76	78	87	92
30/07/2009	13	17	19	24	25	30

which can be compared to the results obtained in the radon balance in the previous section.

On 03 July 2009, the radon and salinity survey extended into a very shallow, hypersaline part of the lagoon. In this shallow part of the lagoon, radon concentrations were elevated over the ocean endmember – the corresponding values lie above the mixing line of ocean water with groundwater in the salinity–radon diagram (Fig. 6a). This radon must originate from sources other than groundwater, i.e. in-situ ^{226}Ra decay, diffusion and/or seawater recirculation. Hypersaline conditions in this zone indicate that lateral mixing in this zone was greatly reduced during this period of observation. The recirculation flux across the sediment–water interface q and the radon concentration of the interstitial water C_i can be calculated as a function of γ from Eqs. (10) and (12) respectively.

At locations with a (measured) water depth of 0.2 m, the total radon concentration in the hypersaline zone ranged between 45 and 65 Bq m^{-3} (lower values in Fig. 6 correspond to locations with greater water depth). Assuming 15 Bq m^{-3} and 5 Bq m^{-3} are due to diffusion and to in-situ ^{226}Ra decay (as measured) respectively, the contribution of seawater recirculation (C in Eqs. (10) and (12)) is the remainder of $25\text{--}45 \text{ Bq m}^{-3}$. Considering an average value of 35 Bq m^{-3} at a (measured) water depth d of 0.2 m, a gas piston velocity k of 1.2 m day^{-1} (as calculated from wind data on 03 July 2009), a typical residence time T of 1 day (based on the daily cycle of water level fluctuations; Fig. 5b), and a γ of $2780 \pm 950 \text{ Bq m}^{-3}$, C_i and q can now be calculated after Eqs. (10) and (12) to be 2385 ($1580\text{--}3190$) Bq m^{-3} and 0.018 ($0.014\text{--}0.028$) m d^{-1} respectively.

This relationship can be compared with the results obtained from the non-steady state radon mass balance. There, a total recirculation flux of $1.6 \times 10^8 \text{ Bq day}^{-1}$ to the northern lagoon was calculated (Table 4), which equates to a unit area flux of radon of $42 \text{ Bq m}^{-2} \text{ day}^{-1}$. A unit area flux of water is obtained by dividing the unit area flux of radon by C_i to be 0.018 ($0.013\text{--}0.027$) m d^{-1} . The two independent models thus yield almost identical results.

It is interesting to note that following Cook et al. (2008), the diffusive flux F_{diff} of radon can be estimated if the radon production rate and effective diffusion coefficient through lagoon sediments are known. At an assumed diffusion coefficient of $2.2 \times 10^{-6} \text{ m}^2 \text{ day}^{-1}$, the diffusive flux is estimated to be $15.4 \pm 5.3 \text{ Bq m}^{-2} \text{ d}^{-1}$, very similar to the diffusion rate calculated following Burnett et al. (2003).

3. Discussion

3.0.1. Sources of radon in La Palme lagoon

3.0.1.1. Low-salinity karstic groundwater discharge. The results of this study illustrate that despite the small volume discharge ($0.8\text{--}1.2\%$ of northern lagoon volume per day) the discharge of low-salinity groundwater provides a significant counterbalance to salinization of the seasonally closed lagoon due to evaporation in the dry summer

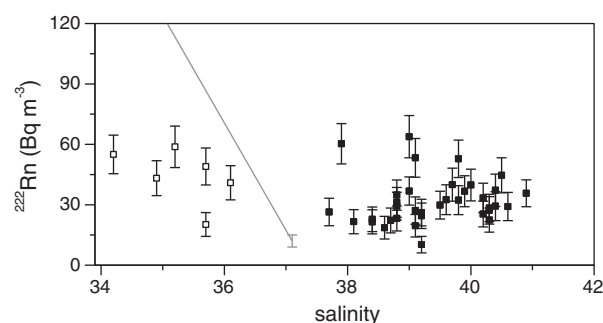


Fig. 6. Salinity–radon relationship in the hypersaline zone of the lagoon. The mixing line between groundwater and ocean water using endmembers shown in Table 1 is shown as a continuous line. Data below the mixing line (open symbols) is from the main lagoon (not the hypersaline zone), and is included for comparison only.

Table 4

Absolute and relative contributions of different sources to the radon budget of La Palme lagoon.

Rn source	Rn flux (10^6 Bq day $^{-1}$)			Relative Rn flux		
	Min	Mean	Max	Min	Mean	Max
Groundwater	27.8	39.9	54.0	7%	11%	18%
Diffusion	44.4	61.1	77.8	11%	17%	26%
^{226}Ra decay	98.1	98.8	99.9	23%	27%	34%
Circulation flux	250.9	159.8	65.2	60%	44%	22%

months, and thus contributes to maintaining transitional (brackish) ecosystem functioning.

Whilst the low-salinity karstic groundwater significantly affects the salinity budget of the lagoon, it contributes only a small fraction of 7–18% of total radon input to La Palme lagoon. This is partially a result of the comparatively low endmember radon concentration of 1600 ± 200 Bq m $^{-3}$, which together with its salinity of 7.3 (Table 1) indicates a mixing of fresh groundwater with seawater in the aquifer, consistent with previous studies of the local karst geochemistry (e.g. Aquilina et al., 2002; Fleury et al., 2007).

The calculated groundwater flux of 0.29 ± 0.05 m 3 s $^{-1}$ is similar to the only previous estimate of groundwater discharge into La Palme lagoon of 0.5 m 3 s $^{-1}$ during the month of July by Wilke and Boutière (2000), whose estimate was based on a water balance of 7 consecutive years (1994–2000). A manual measurement across the outflow of the lavoire (captured spring) on 26 June 2009 using a basic drifter yielded an outflow from the lavoire of 0.04 m 3 s $^{-1}$, suggesting that the majority of the groundwater flow originates from other point or non-point sources in the wetland on the northern bank of the lagoon. An airborne infrared of the northernmost part of the lagoon image collected in September 2012 is consistent with this observation – it indicates only a small zone of reduced temperature due to discharge from the lavoire's stream at that period of the year (Fig. 7). No other groundwater sources elsewhere in the lagoon other than those in the northern section were identified from the radon or salinity distribution (Fig. 2).

This result is obtained based on the assumption that the lagoon volume (i.e. water level) is constant over the one-month observation period. The comparatively large wind-driven variations in water level mask long-term water level variations and the available water level measurement do not allow for an accurate determination of absolute lagoon water level and volume at any time. Wilke and Boutière (2000) however suggest that lagoon water level (and corresponding volume) can reduce by as much as 10 cm per month in the summer months, due to evaporative loss exceeding water inputs. It is interesting to note that if such a drop in water level of 10 cm and a corresponding reduction in volume were considered in the water balance (Eq. (2)), then a smaller groundwater flux of 0.10 ± 0.06 m 3 s $^{-1}$ would be obtained – very close to the manual measurement of 0.04 m 3 s $^{-1}$ at the outflow of the lavoire. In this case, the relative contribution of groundwater to the radon budget would be smaller, and the contribution of seawater recirculation correspondingly larger. The constant water level assumption used here is thus considered the 'conservative' case, in the sense that more radon is provided by groundwater and less by recirculation, which is the overwhelming contributor (see below). It is clear that it will be of critical importance to accurately measure volumes and water levels in future studies.

3.0.1.2. Temporal variability of lagoon radon concentration. The non-steady state model of lagoon radon concentration describes the observations well, and the overall trend is well captured by the model (Fig. 5). The largest departure of model and data is observed on 30 July, but remains below a 25% difference (Table 3). On 26 June, the average radon concentration was elevated after a period of low wind speed, resulting in reduced gas loss (Fig. 5); on 03 July, wind and water level variations are minimal, and conditions are close to a steady state. This

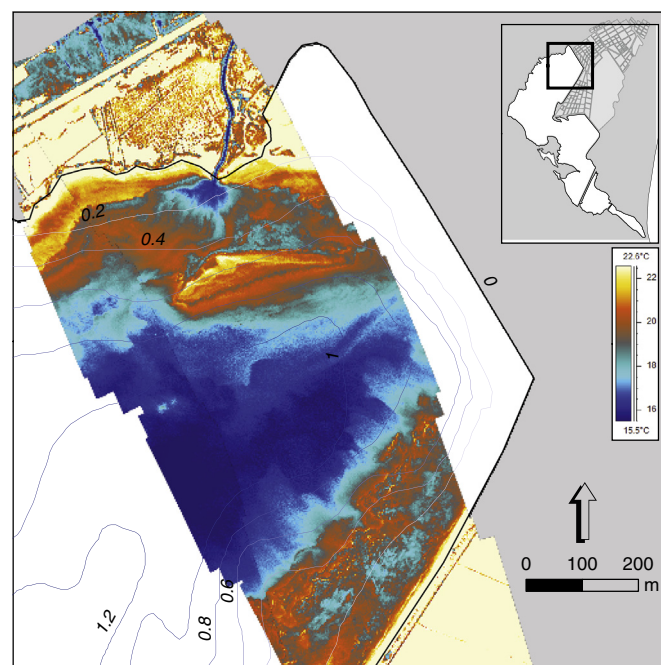


Fig. 7. Airborne infrared image of temperature plume recorded on 20 Sept 2012 at 09:30. It shows a stream that drains a wetland and a captured spring ('lavoire'), supplied by karstic groundwater in the northern section of the lagoon. The temperature distribution indicates only a small spatial influence of discharge on surface temperature in the order of 100 m range, at a water depth of less than 0.3 m.

is also evident in a homogenous spatial radon and salinity gradient on this date which would be expected for steady state conditions (Fig. 2). On 15 July, concentrations are again slightly elevated during a period of low wind speed, and on 30 July, average concentration is the lowest of the four measurements (and the lowest modelled concentration for the entire period), due to a sharp increase in wind speed and associated substantial gas loss.

The measured and modelled lagoon-averaged radon concentration during the observation period June–July 2009 is $19\text{--}76$ Bq m $^{-3}$ and $19\text{--}113$ Bq m $^{-3}$ respectively (Table 3; Fig. 5). This considerable range in variability on daily time scales is comparable to variations observed in other closed aquatic systems (e.g. Burnett and Dimova, 2012). Evident from the model results, the variability is due to an interaction of the two main drivers of radon in the lagoon, i.e. gas loss, the dominant loss term for radon, typical for shallow water bodies (e.g. Cook et al., 2006), and recirculation flux, the dominant source term (Table 4). Although wind speed and water level, the drivers of gas loss and recirculation flux respectively are related in La Palme lagoon, the time lag between wind and water level setup results in a complex pattern in temporal radon variability.

Whilst with 8–15 days the temporal resolution of sampling is low in comparison with other studies, similar observations over a one-month period are rare. In order to assess temporal variability of processes, a temporally extended observation period is often required, and the approach taken here appears to be adequate to capture seasonal lagoon conditions. Frequently, radon budgets are constructed from time series recorded at single points, assuming that the chosen location is representative for the water body (e.g. Burnett and Dulaiova, 2003; Burnett & Dimova, 2012). In this study, a different approach was taken by measuring and modelling a volumetric average. It would have been very difficult to define one point in the lagoon that could have been considered representative for the entire lagoon. In summary, spatially distributed sampling at low temporal resolution is considered a valuable alternative approach to understand water exchange processes in complex coastal systems.

3.0.1.3. Wind-driven recirculation of seawater through lagoon sediments – a major source of radon. The wind-driven advective recirculation flux of radon from sediments F_{recirc} is with 22–60% the largest contributor to the radon budget of the lagoon (Table 4). Assuming a source concentration for the seawater recirculation flux similar to that of groundwater of $1600 \pm 200 \text{ Bq m}^{-3}$ (a common assumption when more detailed data is not available and when groundwater and recirculation fluxes are not distinguished, e.g. Burnett and Dimova, 2012), a water flux of $1.2 (0.4\text{--}2.1) \text{ m}^3 \text{ s}^{-1}$ or $3.9 (1.4\text{--}7.0) \% \text{ day}^{-1}$ of lagoon volume can be calculated. This equates to ca. 4 times the water flux from low-salinity groundwater.

The results from the independent estimation of seawater recirculation via the Cook et al. (2006) hyporheic exchange approach yield very similar results to the mass balance. This additional, independent approach to constrain the input of radon from seawater recirculation through sediments thus provides additional confidence in the results obtained in the mass balance.

In summary, the results of the study demonstrate that seawater recirculation is a major contributor to total radon and water fluxes to the lagoon. Using a stand-alone radon model would have significantly overestimated the flux of groundwater of karstic origin.

3.0.2. Radon & salinity distribution in Salses-Leucate & Thau lagoons

Data collected in Salses-Leucate and Thau lagoons is insufficient to construct similar solute balances. However, the collected radon and salinity data allows for a qualitative assessment of contributing processes also in these lagoons.

In Salses-Leucate lagoon, salinity remained well below seawater salinity along the transects, and radon and salinity are significantly affected by groundwater discharge from the karst springs Font Dame and Font Estramar in the SW sector (Fig. 4). These springs are some orders of magnitude greater in flow rate than the discharge observed at La Palme lagoon, with reported flow rates of Font Estramar and Font Dame of $1\text{--}15 \text{ m}^3 \text{ s}^{-1}$ and $1\text{--}5 \text{ m}^3 \text{ s}^{-1}$ respectively (Fleury et al., 2007).

Previous reports and anecdotal evidence suggest there may be additional connections of the karst aquifer to the lagoons, in particular in the northern part of Salses-Leucate lagoon (e.g. Ladouche et al., 2000). Local fishermen report distinct zones in Leucate lagoon that did not freeze in winter, when the lagoon had no opening to the ocean ca. 25 years ago and was of significantly lower salinity than today. This was inferred to result from discharge of relatively warm groundwater in winter. The spatial distribution of radon and salinity observed in 2009 suggests however that the two major springs are the main drivers of radon and salinity distribution in the lagoon. In addition, groundwater input from small springs adjacent to a fishing village in the south-western section results in slightly elevated radon concentration and slightly reduced salinity (Fig. 4).

In contrast, concurrent radon-salinity surveys in Thau lagoon indicate that summer surface water is not greatly affected by direct groundwater flow from low-salinity groundwater (Fig. 4). In the northernmost bay, radon is slightly elevated, presumably due to radon input from the well-known spring La Vise in this sector (Fig. 4). The groundwater flow rate of La Vise is in the order of a few 100 l s^{-1} (Fleury et al., 2007), and discharges at ca. 30 m of water depth, so would not be expected to play an important role in radon and salinity budget of the lagoon. The observed ^{222}Rn concentration of 2040 Bq m^{-3} of La Vise can be compared with ^{222}Rn activities recently reported by Condomines et al. (2012) in waters collected in wells located in the adjacent area of Balaruc-les-Bains. Waters of different origins can be found in the hydrological system of Balaruc-les-Bains: karstic waters, thermal waters, seawater in-flow either from the coastal sea or from the lagoon (Condomines et al., 2012; Ladouche et al., 2012). Activities of up to $26\,000 \text{ Bq m}^{-3}$ were found in karstic waters whereas deep thermal waters displayed activities of 1900 Bq m^{-3} (Condomines et al., 2012). The relatively moderate ^{222}Rn concentration determined at the outlet of La Vise at a

salinity of 1.4 thus suggests a deep thermal source at the time of sampling, without a substantial contribution of seawater.

The highest radon concentrations and lowest salinity in surface waters were found in the Canal de Midi which is connected to the lagoon, and subject to flow regime and wind direction may contribute significantly to the radon and salinity budgets of the lagoon.

In addition, a further source of radon is evident in shallow sections of the lagoon from its elevated radon signature 'above' the mixing line between ocean and groundwater (Fig. 8). Similar to La Palme lagoon, wind-driven pumping of seawater through sediments and/or diffusion can explain the systematic elevation in radon concentration in shallow parts of Thau lagoon. Two distinctly different zones are evident in Fig. 8 – one on the shallow north and south shores, and one in the port of Sète. From their particular spatial distribution, it is suggested that elevated radon in the shallow sections is primarily due to wind-driven seawater recirculation through the shallow sediment similar to the observations in La Palme lagoon. The elevated concentrations found in the port are perhaps more likely due to diffusive fluxes in this sheltered port which – at small tides – would be characterised by comparatively high residence times, at the same time reduced wind effects allowing for an accumulation of diffusive fluxes. Inspection of the mixing diagram from Thau lagoon thus indicates that the processes documented in La Palme lagoon are unlikely to be restricted to La Palme lagoon, and are also likely to occur in other lagoons.

In summary, it has been shown that the concurrent collection of radon and salinity data provides a useful tool to qualitatively and quantitatively assess water exchange processes in coastal lagoons. It allowed for the mapping of different radon source processes in Thau lagoon, and for a quantitative determination of recirculation fluxes in La Palme lagoon. It is suggested that in future studies salinity data is always collected and interpreted in combination with radon data in closed or semi-closed coastal systems.

3.0.3. Biogeochemical and lagoon management implications

Whilst of critical importance to the salinity regime of La Palme (and Salses-Leucate), low-salinity groundwater discharge plays a comparatively small role in the radon budget of La Palme (and Thau) lagoons. Together with radon dissolved in groundwater, biogeochemically relevant solutes can be transported in groundwater or recirculated seawater (Burnett et al., 2006; Moore, 2010). The significant contributions of the recirculation flux to the radon budget strongly suggest that other solutes such as nutrients or contaminants may also be transported with this wind-driven recirculation flux. Nutrient and contaminant enrichment of sediments in Mediterranean lagoons is well documented, in particular of phosphorus (De Casabianca et al., 1997) and a range of bio-available toxins (Galgani et al., 2009). Incidentally, the shallow part of Thau lagoon where seawater recirculation is here suggested to potentially occur is characterised by above-average levels of sediment toxicity as measured with oyster bioassays (Galgani et al., 2009). Wind-driven seawater recirculation through lagoon sediments documented in this study may remobilise nutrients and contaminants, but in current models of biogeochemical budgets of the investigated and of other lagoons, this advective recirculation process is not considered to date (e.g. Plus et al., 2006).

4. Conclusions

In Salses-Leucate lagoon, discharge of groundwater from the regional karst aquifer modifies lagoon salinity and radon concentration, which is a tracer for water and solute exchanges across the sediment-water interface. In contrast, in La Palme and Thau lagoons, low-salinity groundwater discharge from the karstic aquifer plays only a minor role in the radon budget during the summer months. Using a stand-alone radon model without considering a water and salt budget would have significantly overestimated the flux of groundwater of karstic origin.

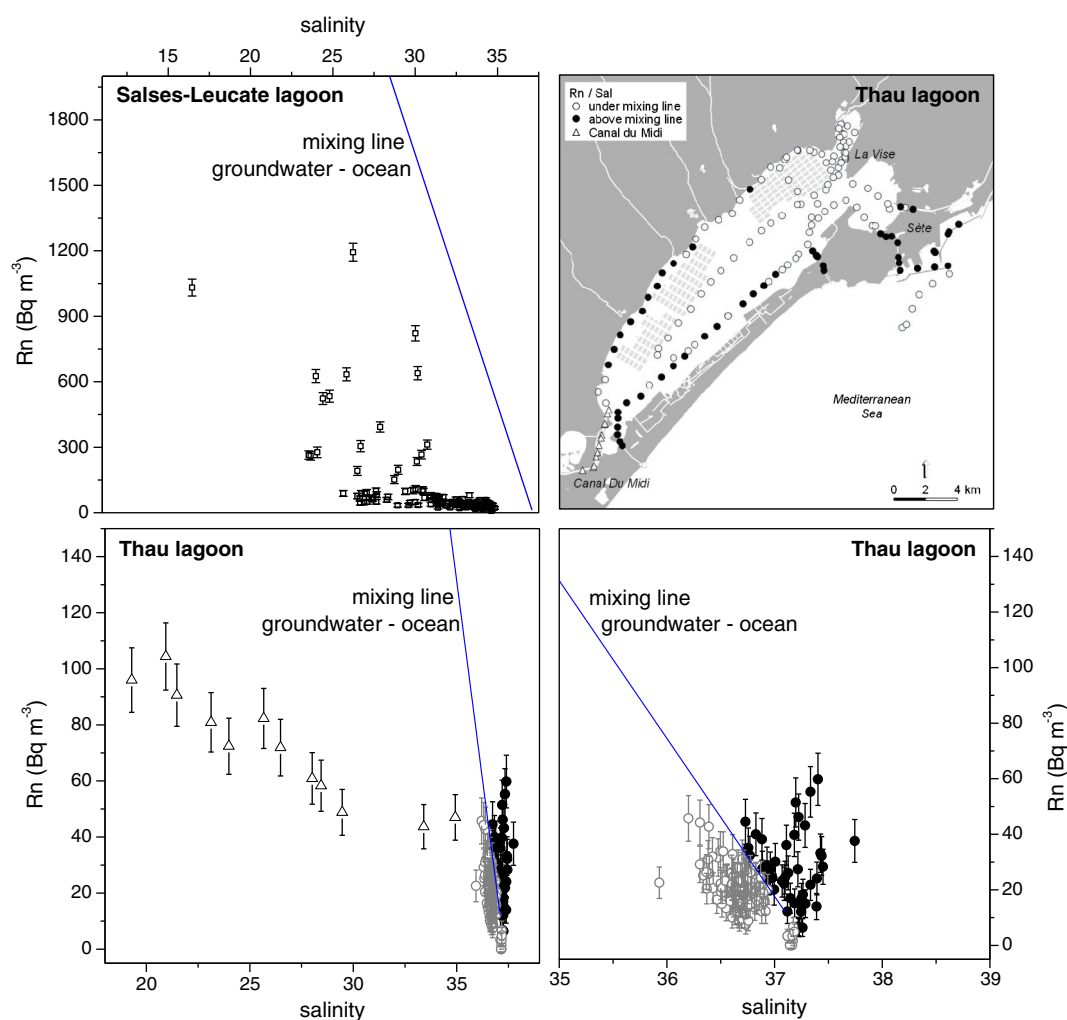


Fig. 8. Salinity–radon mixing diagrams of Salses-Leucate (top left) and Thau (bottom row; same data on both diagrams) lagoons. The map of Thau lagoon (top right) shows data classified by type identified from the mixing diagram: samples that lie above the mixing line on groundwater with ocean water are marked with black dots in mixing diagrams and map.

Wind-driven seawater recirculation through sediments is with 44% (22–60%) the largest source of radon to La Palme lagoon, and may also make significant contributions to the shallow parts of Thau lagoon. In other words, in the small La Palme lagoon, on average every 25 days the equivalent of the volume of the entire lagoon recirculates through the sediment. This recirculation of lagoon water through sediments may be an additional process in the transport of nutrients and contaminants to the lagoons through remobilisation from lagoonal sediments. It may thus play a significant role in lagoonal biogeochemical budgets, and, subject to further study, may require consideration in water quality management in French coastal lagoons.

Author contributions

PvB & TS conceived the study; TS, PvB & MS carried out the field sampling and analyses; TS & PC carried out the modelling and TS wrote the paper.

Acknowledgements

For their support of this study, we thank T Laugier & J Barret (IFREMER Sète), B Troqueraud & F Nivelet (Capitainerie de Leucate), K Fortuné-Sans (Parc naturel régional de la Narbonnaise en Méditerranée), L Fonbonne (Syndicat mixte RIVAGE Salses-Leucate) and L & N Fouré (Cap D'Adge). S Jullien & S Cockenpot, A Radic (LEGOS), S Thomas

(IUEM Brest), P Brunet & JL Seidel (Hydrosiences Montpellier), T. Laugier & J Barret (IFREMER Sète) provided helping hands in the field. M Bakalowicz (Hydrosiences Montpellier) and P Fleury (BRGM Montpellier) shared their local knowledge prior to data collection. A Dujon and S Hervé (IUEM, Brest) provided support with data analysis and the graphical abstract respectively.

The project was partially funded by the 'Fondation de Coopération Scientifique Sciences et Technologies pour l'Aéronautique et l'Espace' through the program CYMENT (Cycle de l'eau et de la matière dans les bassins versants) to PvB. Radon sampling equipment was funded by ARC Discovery Grant DP0209526 and James Cook University to TS. The acquisition of the thermal infrared images was performed by TCC (Beauvais) in the framework of the Tosca-Geomether project funded by the Centre National d'Etudes Spatiales CNES. TS' visit at LEGOS was funded by the Centre national de la recherche scientifique CNRS (poste rouge). TS is currently visiting the Laboratoire des sciences de l'environnement marin UMR 6539, Plouzané, France as a senior European Union FP7 International Incoming Fellow. R Doble, S Lamontagne and J Turner (CSIRO, Australia) commented on an early draft, and constructive comments from two anonymous reviewers are appreciated.

References

- Andral, B., Sargian, P., 2010. Directive Cadre Eau – Contrôles de Surveillance/Opérationnel District 'Rhône et Cotiers Méditerranéens' Campagne DCE 2009 (RST.DOP/LER-PAC/10-19).

- Anonymous, 2007. Operation de restauration hydraulique de la partie sud de l'Etang de La Palme. Dossier technique. Parc naturel régional de la Narbonnaise (http://www.pole-lagunes.org/ftp/Dossiertechniq_lapalme_1720Ko.pdf).
- Aquilina, L., Ladouche, B., Doerfliger, N., Seidel, J.L., Bakalowicz, M., Dupuy, C., Le Strat, P., 2002. Origin, evolution and residence time of saline thermal fluids (Balaruc springs, southern France): implications for fluid transfer across the continental shelf. *Chem. Geol.* 192, 1–21.
- Beklioglu, M., Romo, S., Kagalogi, I., Quintana, X., Bécarea, E., 2007. State of the art in the functioning of shallow Mediterranean lakes, workshop conclusions. *Hydrobiologia* 584, 317–326. <http://dx.doi.org/10.1007/s10750-007-0577-x>.
- Burnett, W.C., Dulaiova, H., 2003. Estimating the dynamics of groundwater input into the coastal zone via continuous radon-222 measurements. *J. Environ. Radioactiv.* 69, 21–35.
- Burnett, W.C., Cable, J.E., Corbett, D.R., 2003. Radon tracing of submarine groundwater discharge in coastal environments. In: Taniguchi, M., Wang, K., Gamo, T. (Eds.), *Land and Marine Hydrogeology*. Elsevier, Amsterdam.
- Burnett, W.C., Aggarwal, P.K., Bokuniewicz, H., Cable, J.E., Charette, M.A., Kontar, E., Krupa, S., Kulkarni, K.M., Loveless, A., Moore, W.S., Oberdorfer, J.A., Oliveira, J., Ozyurt, N., Povinec, P., Privitera, A.M.G., Rajar, R., Ramessur, R.T., Scholten, J., Stieglitz, T., Taniguchi, M., Turner, J.V., 2006. Quantifying submarine groundwater discharge in the coastal zone via multiple methods. *Sci. Total Environ.* 367, 498–543.
- Burnett, W.C., Dimova, N., 2012. A radon-based mass balance model for assessing groundwater inflows to lakes. In: Taniguchi, M., Shiraiwa, M. (Eds.), *The Dilemma of Boundaries: Toward a New Concept of Catchment*, Global Environmental Studies. Springer, Japan, pp. 55–66. http://dx.doi.org/10.1007/978-4-431-54035-9_6.
- Cook, P.G., Favreau, G., Dighton, J.C., Tickell, S., 2003. Determining natural groundwater inflow to a tropical river using radon, chlorofluorocarbons and ionic environmental tracers. *J. Hydrol.* 277, 74–88.
- Cook, P.G., Lamontagne, S., Berhane, D., Clark, J.F., 2006. Quantifying groundwater discharge to Cockburn River, southeastern Australia, using dissolved gas tracers ^{222}Rn and SF_6 . *Water Resour. Res.* 42, W10411. <http://dx.doi.org/10.1029/2006WR004921>.
- Cook, P.G., Wood, C., White, T., Simmons, C.T., Fass, T., Brunner, P., 2008. Groundwater inflow to a shallow, poorly-mixed wetland estimated from a mass balance of radon. *J. Hydrol.* 354, 213–226.
- Condomines, M., Gourdin, E., Gataniau, D., Seidel, J.L., 2012. Geochemical behaviour of Radium isotopes and Radon in a coastal thermal system (Balaruc-les-Bains, South of France). *Geochim. Cosmochim. Acta* 98, 160–176.
- De Casabianca, M.L., Laugier, T., Marinho-Soriano, E., 1997. Seasonal changes of nutrients in water and sediment in a Mediterranean lagoon with shellfish farming activity (Thau Lagoon, France). *ICES J. Mar. Sci.* 54, 905–916.
- Fleury, P., Bakalowicz, M., de Marsily, G., 2007. Submarine springs and coastal karst aquifers: a review. *J. Hydrol.* 339, 79–92.
- Galgani, F., Senia, J., Guillou, J.L., Laugier, T., Munaron, D., Andral, B., Guillaume, B., Coulet, E., Boissery, P., Brun, L., Bertrand, M.C., 2009. Assessment of the environmental quality of French continental Mediterranean lagoons with oyster embryo bioassay. *Arch. Environ. Contam. Toxicol.* 57 (3), 540–551.
- Garcia-Solsona, E., Garcia-Orellana, J., Masqué, P., Rodellas, V., Mejías, M., Ballesteros, B., Domínguez, J.A., 2010. Groundwater and nutrient discharge through karstic coastal springs (Castelló, Spain). *Biogeosci. Discuss.* 7, 631–669.
- Johannes, R.E., 1980. The ecological significance of submarine discharge of groundwater. *Mar. Ecol. Prog. Ser.* 3, 365–373.
- Johannes, R.E., Hearn, C.J., 1985. The effect of submarine groundwater discharge on nutrient and salinity regimes in a coastal lagoon off Perth, Western Australia. *Estuar. Coast. Shelf Sci.* 21 (6), 789–800.
- Kim, G., Hwang, D.W., 2002. Tidal pumping of groundwater into the coastal ocean revealed from submarine ^{222}Rn and CH_4 monitoring. *Geophys. Res. Lett.* 29 (14), 1678. <http://dx.doi.org/10.1029/2002GL015093>.
- Kjerfve, B., 1994. *Coastal Lagoon Processes*. Elsevier, Amsterdam.
- Ladouche, B., LeBec, C., Aquilina, L., Bakalowicz, M., Souchu, P., Doerfliger, N., Anus, S., 2000. Recherche de l'origine de la contamination bactériologique de l'étang de Salses Leucate (Rap BRGM/RP-50003-FR).
- Ladouche, B., Millot, R., Guerrot, C., Lamotte, C., 2012. Caractérisation géochimique de l'aquifère hydrothermal de Balaruc-les-Bains lors d'un épisode d'inversac. Dix-huitième journées techniques du Comité Français d'Hydrogéologie de l'association internationale des Hydrogéologues. Ressources et gestion des aquifères littoraux, Cassis.
- MacIntyre, S., Wanninkhof, S.R., Chanton, J.P., 1995. Trace gas exchange across the air-sea interface in freshwater and coastal marine environments. In: Matson, P.A., Harris, R.C. (Eds.), *Biogenic Trace Gases: Measuring Emissions from Soil and Water*. Blackwell Science, London, pp. 52–97.
- Martínez-Alvarez, V., Gallego-Elvira, B., Maestre-Valero, J.F., Tanguy, M., 2011. Simultaneous solution for water, heat and salt balances in a Mediterranean coastal lagoon (Mar Menor, Spain). *Estuar. Coast. Shelf Sci.* 91 (2), 250–261.
- Moore, W.S., 2010. The effect of submarine groundwater discharge on the ocean. *Ann. Rev. Mar. Sci.* 2, 59–88.
- Obrador, B., Moreno-Ostos, E., Pretus, J.L., 2008. A dynamic model to simulate water level and salinity in a Mediterranean coastal lagoon. *Estuar. Coasts* 31 (6), 1117–1129.
- Plus, M., La Jeunesse, I., Bouraouic, F., Zaldívar, J.M., Chapellet, A., Lazuref, P., 2006. Modelling water discharges and nitrogen inputs into a Mediterranean lagoon Impact on the primary production. *Ecol. Model.* 193 (1–2), 69–89. <http://dx.doi.org/10.1016/j.ecolmodel.2005.07.037>.
- Povinec, P.P., Bokuniewicz, H., Burnett, W.C., Cable, J., Charette, M., Comanducci, J.F., Kontar, E.A., Moore, W.S., Oberdorfer, J.A., de Oliveira, J., Peterson, R., Stieglitz, T., Taniguchi, M., 2008. Isotope tracing of submarine groundwater discharge offshore Ubatuba, Brazil: results of the IAEA-UNESCO SGD project. *J. Environ. Radioact.* 99 (10), 1596–1610.
- Povinec, P.P., Comanducci, J.F., Levy-Palomo, I., Oregioni, B., 2006. Monitoring of submarine groundwater discharge along the Donnalucata coast in the south-eastern Sicily using underwater gamma-ray spectrometry. *Cont. Shelf Res.* 26, 874–884.
- Rapaglia, J., Ferrarin, C., Zaggia, L., Moore, W.S., Umgieser, G., Garcia-Solsona, E., Garcia-Orellana, J., Masqué, P., 2009. Investigation of residence time and groundwater flux in Venice Lagoon: comparing radium isotope and hydrodynamical models. *J. Environ. Radioact.* 101, 571–581. <http://dx.doi.org/10.1016/j.jenvrad.2009.08.010>.
- Rodellas, V., Garcia-Orellana, J., Garcia-Solsona, E., Masqué, P., Domínguez, J.A., Ballesteros, B.J., Mejías, M., 2012. Quantifying groundwater discharge from different sources into a Mediterranean wetland by using ^{222}Rn and Ra isotopes. *J. Hydrol.* 466–467, 11–22. <http://dx.doi.org/10.1016/j.jhydrol.2012.07.005>.
- Rodríguez-Rodríguez, M., Moreno-Ostos, E., 2006. Heat budget, energy storage and hydrological regime in a coastal lagoon. *Limnologia* 36, 217–227.
- Schubert, M., Paschke, A., Bednorz, D., Bürkin, W., Stieglitz, T., 2012. Kinetics of the water/air phase transition of radon and its implication on detection of radon-in-water concentrations: practical assessment of different on-site radon extraction methods. *Environ. Sci. Technol.* 46 (16), 8945–8951. <http://dx.doi.org/10.1021/es3019463>.
- Schubert, M., Paschke, A., Lieberman, E., Burnett, W.C., 2012. Air–water partitioning of ^{222}Rn and its dependence on water temperature and salinity. *Environ. Sci. Technol.* 46 (7), 3905–3911. <http://dx.doi.org/10.1021/es204680n>.
- Slomp, C.P., Van Cappellen, P., 2004. Nutrient inputs to the coastal ocean through submarine groundwater discharge: controls and potential impact. *J. Hydrol.* 295, 64–86.
- Smith, S.V., Marshall-Crossland, J.L., Crossland, C.J., 1999. Mexican and Central American coastal lagoon systems: carbon, nitrogen and phosphorus fluxes (regional workshop II). LOICZ Reports & Studies No. 13. LOICZ IPO, Texel, The Netherlands (ii + 115 pp.).
- Spaulding, M.L., 1994. Modeling of circulation and dispersion in coastal lagoons. In: Kjerfve, B. (Ed.), *Coastal Lagoon Processes*. Elsevier, Amsterdam, pp. 103–131.
- Stieglitz, T.C., Cook, P.G., Burnett, W.C., 2010. Inferring coastal processes from regional-scale mapping of ^{222}Rn and salinity: examples from the Great Barrier Reef, Australia. *J. Environ. Radioact.* 101, 544–552.
- Troussellier, M., Bacher, C., 2006. Mediterranean lagoons worksite. In: Clavier, J., Joanny, M., Carlotti, F. (Eds.), *The French Coastal Environmental Research Programme: Overview of 1999–2002*. Editions Quae, Paris.
- van Beek, P., Souhaut, M., Reyss, J.L., 2010. Measuring the radium quartet (^{228}Ra , ^{226}Ra , ^{224}Ra , ^{223}Ra) in seawater samples using gamma spectrometry. *J. Environ. Radioact.* 101 (7), 521–529.
- Viaroli, P., Mistri, M., Troussellier, M., Guerzoni, S., Cardoso, A.C., 2005. Structure, functions and ecosystems alterations in Southern European coastal lagoons: preface. *Hydrobiologia* 550, 7–9.
- Wanninkhof, R., Asher, W.E., Ho, D.T., Sweeney, C., McGillis, W.R., 2009. Advances in quantifying air–sea gas exchange and environmental forcing. *Annu. Rev. Mar. Sci.* 1, 213–244.
- Wilke, M., Boutière, H., 2000. Synthèse générale du fonctionnement hydrobiologique de l'étang de La Palme. CEH, Perpignan.
- Zaldívar, J.M., Cardoso, A.C., Viaroli, P., Newton, A., de Wit, R., Ibañez, C., Reizopoulou, S., Somma, F., Razinkovas, A., Basset, A., Holmer, M., Murray, N., 2008. Eutrophication in transitional waters: an overview. *Transit Waters Monogr.* 1, 1–78.